Performance of Turbo Equalization using Doped Accumulator with Channel Estimation

Yasuhiro Takano*, Khoirul Anwar*, and Tad Matsumoto*§.
* Japan Advanced Institute of Science and Technology (JAIST), 1-1 Asahidai, Nomi, Ishikawa, 923-1292 JAPAN
Email: {yace.takano, anwar-k, matumoto}@jaist.ac.jp
§ Centre for Wireless Communications, University of Oulu, FI-90014 Finland
Email: tadashi.matsumoto@ee.oulu

***Abstract*—The major objective of this paper is to reveal the performance of the turbo equalization using doped accumulator (TEQ-ACC) when it is combined with channel estimation, in broadband single carrier signalling. It is shown that the accuracy of the channel estimate in TEQ-ACC is inferior to that in conventional turbo equalization (TEQ-CVT), if TEQ-ACC generates the soft replica only from the soft information fed back from the decoder. To cope with this problem, this paper proposes a new soft replica generation method for TEQ-ACC which achieves asymptotically the equivalent accuracy of channel estimates to that with TEQ-CVT. Simulation results show that the gain in frame-error-rate (FER) with TEQ-ACC utilizing the proposed soft replica generation method is significant, 1 dB better than TEQ-CVT at FER = 10^{-3} under pedestrian mobility channel assumptions. Furthermore, this paper verifies that TEQ-ACC with channel estimation implemented by an adaptive subspace tracking technique, Low rank adaptive filtering (LORAF), achieves exactly the same FER performance as that with the sliding window singular value decomposition (SVD)-based technique.**

I. Introduction

It is well-known that turbo equalization with doped accumulator achieves significant gain in terms of bit-error-rate (BER) over the conventional techniques that do not use the doped accumulator [1] [2], even though the channel codes in the both techniques have the same memory length in total (i.e., channel encoder plus doped accumulator). However, majority of literatures on turbo equalization assume that the channel impulse response is known, and performance comparison between turbo equalization with and without the doped accumulator when it combined with channel estimator is not well studied.

Hence, the major objective of this paper is to reveal the performance of the turbo equalization using doped accumulator (TEQ-ACC) when it is combined with the channel estimation. This paper makes performance comparison between TEQ-ACC and the conventional turbo equalization (TEQ-CVT) in single carrier signalling. In both TEQ-ACC and TEQ-CVT, the total memory length due to channel encoder plus doped accumulator is kept the same for fair comparison. Doping may degrade the channel estimation accuracy because the decoder in TEQ-ACC does not feed back the log-likelihood ratio of the doped bits, which motivates this work. This paper proposes a new soft replica generation method for channel estimation in TEQ-ACC to reduce such negative effect of doping. This paper investigates the accuracy of channel estimation on TEQ-ACC in a realistic propagation scenario based on measurement data as well as in the model-based frequency selective fading channel through computer simulations. Furthermore, this paper verifies the frame-error-rate (FER) performance of TEQ-ACC when it is combined with a channel estimation technique using subspace tracking algorithms LORAF1 and LORAF3 [3] in realistic propagation scenarios.

This paper is organized as follows. *Section II* describes the system model assumed in this paper. *Section III* proposes a new soft replica generation method, effective with the doped accumulator, for the channel estimation in turbo equalization. *Section IV* describes the impact on the convergence property of the doped accumulator when it is combined with the channel estimation. *Section V* presents results of computer simulations. This paper is concluded in *Section VI* with concluding remarks.

Notations

The bold upper-case $\mathbf{X}$ and lower-case $\mathbf{x}$ denote a matrix and a vector, respectively. $\mathbf{X}^H$ denotes the transposed conjugation of the matrix $\mathbf{X}$. $\mathtt{diag}(\mathbf{X})$ is a function to form a vector with the diagonal elements of the matrix $\mathbf{X}$. $\mathbf{X}|_{1:r}$ is a submatrix composed of the first r column vectors in $\mathbf{X}$.

II. System Model

Binary information $b(i)$, $1 \leq i \leq N_d N_B$, is encoded by a rate R_c convolutional code (CC) with a generator polynomial $(g_1, \cdots, g_{1/R_c})$ and is interleaved by an interleaver (Π). The output $c(k)$ is further encoded into $a(k)$ by the doped accumulator (ACC). The sequence $a(k)$ is divided into N_B bursts such that fading is assumed to be static over each block. The transmitter transmits $N_d/(2R_c)$ Gray mapped quadrature phase shift keyed (QPSK) symbols $x(k_s; l)$ together with training symbols and the cyclic prefix (N_t and N_{CP} symbols, respectively) using the single carrier signalling, where k_s and l denote the symbol and the burst indexes, respectively.

This work was supported in part by the Japanese government funding program (Grant-in-Aid for Scientific Research (B), No. 23360170), and in part by the Mobile Radio Center (MRC) foundation.

978-1-4577-1180-0/11/$26.00

The receiver receives the signal $y(k_s;l)$ suffering from inter symbol interference (ISI) due to frequency selective fading, of which channel memory length is up to W symbols. The received signal also suffers from complex additive white Gaussian noise (AWGN) $z(k_s) \sim \mathcal{CN}(0, \sigma_z^2)$, as

$$y(k_s;l) \quad = \quad \sum_{t=1}^{W} x(k_s - t + 1; l) \cdot h(t;l) + z(k_s) \qquad (1)$$

with $h(t;l)$ being the channel impulse response. We stack the terms on the both sides of (1) to re-write the input-output relationship in a vectorized form, as

$$\mathbf{y}(l) \quad = \quad \mathbf{X}(l)\mathbf{h}(l) + \mathbf{z} \qquad (2)$$

for the l-th burst, where $\mathbf{X}(l) \in \mathbb{C}^{K \times W}$ is a Toeplitz matrix with $K = N_d/(2R_c) + N_t + N_{CP}$. As depicted in Fig. 1, the receiver performs the channel estimation (EST) while also obtains the extrinsic log-likelihood ratio (LLR) λ^e_{EQU} corresponding to the transmitted sequence $x(k_s;l)$ by means of the frequency domain soft-cancellation and minimum mean square error (SC-MMSE) turbo equalization [4] (EQU). The channel decoder (CC^{-1}) performs decoding using the LLR $\lambda^a_{DEC} = \lambda^e_{ACC}$, taking into account the LLR update by the de-accumulator (ACC^{-1}), and outputs the *a posteriori* LLR (λ^p_{DEC}) corresponding to $c(i)$ which is used to generate the soft replica. CC^{-1} obtains the estimates of the transmitted sequence $\hat{\mathbf{b}}$ by making hard decision on decoder's *a posteriori* LLR λ^p_{DEC} corresponding to $b(i)$ after several iterations.

EST and EQU utilize the the soft replica of transmitted symbols $\bar{\mathbf{x}}_{d,EST}$ and $\bar{\mathbf{x}}_{d,EQU}$, respectively. $\bar{\mathbf{x}}_{d,EST}$ is generated from the *a priori* LLR for channel estimation λ^a_{EST} after interleaving the *a posteriori* LLR λ^p_{DEC}. On the other hand, $\bar{\mathbf{x}}_{d,EQU}$ is generated from the equalizer's *a priori* LLR λ^a_{EQU} which is the interleaved version of extrinsic LLR $\lambda^e_{DEC} = \lambda^p_{DEC} - \lambda^a_{DEC}$, according to the turbo principle.

Note that, as described in [1], the doped accumulator is a recursive memory 1 convolutional coder that outputs at the every P_a-th bit timings the parity bits and otherwise systematic (un-accumulated) bits. At the receiver side, the de-accumulator updates the extrinsic LLR λ^e_{EQU} output from the equalizer by using the Bahl, Cocke, Jelinek and Raviv (BCJR) algorithm [5], while also exploiting *a priori* LLR $\lambda^a_{EQU} = \lambda^e_{DEC}$ fed back from the decoder.

III. Channel Estimation Techniques

In this section, we review the channel estimation techniques to provide better understanding of the convergence property of turbo equalization in *Section* IV. We then propose a new method for generating soft replica to be used in the channel estimator as a reference signal in TEQ-ACC.

A. Review of Channel Estimation Techniques

1) Single Burst ML Channel Estimation: The single burst maximum likelihood (ML) channel estimation (SB_ML) [6] is reduced to (3) with (4) and (5).

$$\hat{\mathbf{h}}^{SB}(l) \quad = \quad \mathbf{R}^{-1}_{\mathbf{XX}}(l)\mathbf{R}_{\mathbf{XY}}(l), \qquad (3)$$

$$\mathbf{R}_{\mathbf{XX}}(l) \quad = \quad \mathbf{X}^H_t(l)\mathbf{X}_t(l) + \gamma(l)\bar{\mathbf{X}}^H_d(l)\bar{\mathbf{X}}_d(l), \qquad (4)$$

$$\mathbf{R}_{\mathbf{XY}}(l) \quad = \quad \mathbf{X}^H_t(l)\mathbf{y}_t(l) + \gamma(l)\bar{\mathbf{X}}^H_d(l)\mathbf{y}_d(l). \qquad (5)$$

$\mathbf{X}_t$ and $\bar{\mathbf{X}}_d$ are Toeplitz matrices for the training and for the soft replica of data symbols, respectively, corresponding to (2). $\gamma(l) = \sigma_z^2/(\sigma_z^2 + \Delta\sigma_d^2(l))$ with $\Delta\sigma_d^2(l) = 1 - \mathrm{E}[||\bar{\mathbf{x}}_d||^2]$.

2) Multiburst Burst ML Channel Estimation: It is also well-known that the multi burst ML channel estimation (MB_ML) [6] improves the estimation accuracy of turbo channel estimation. MB_ML can be approximated by (6) under the assumption that the transmitted symbols are random and long enough:

$$\hat{\mathbf{h}}^{MB}(l) \quad \approx \quad \hat{\mathbf{P}} \cdot \hat{\mathbf{h}}^{SB}(l)\,. \qquad (6)$$

The projection matrix $\hat{\mathbf{P}}$ is given by $\hat{\mathbf{P}} = \hat{\mathbf{U}}_r\hat{\mathbf{U}}^H_r$, where $\hat{\mathbf{U}}_r = \mathbf{U}|_{1:\hat{r}}$ is composed of the first r significant column eigenvectors of $\mathbf{C}_{\hat{\mathbf{h}}}$ (sample covariance matrix of $\hat{\mathbf{h}}$ for the last L bursts), as

$$\mathbf{C}_{\hat{\mathbf{h}}} \quad = \quad \frac{1}{L}\sum_{i=l-L+1}^{l} \hat{\mathbf{h}}^{SB}(i)\left(\hat{\mathbf{h}}^{SB}(i)\right)^H, \qquad (7)$$

$$\mathbf{U}\Sigma\mathbf{V} \quad = \quad \mathtt{svd}\left(\mathbf{C}_{\hat{\mathbf{h}}}\right). \qquad (8)$$

The number of the significant eigenvectors can be predicted by using the minimum description length (MDL) [7] for the singular values of $\mathbf{C}_{\hat{\mathbf{h}}}$, as

$$\hat{r} \quad = \quad \underset{r \le r_{max}}{\arg\min}\, \mathrm{MDL}\{\mathtt{diag}(\Sigma)|_{1:r}\} \qquad (9)$$

with a pre-defined constant $r_{max} \le W$. The computational complexity required for performing the singular value decomposition (SVD) in (8) is $O(W^3)$ [8]. To reduce the complexity, the projection matrix $\hat{\mathbf{P}}$ can be recursively updated by the subspace tracking techniques such as LORAF [3], as proposed in [9]. The LORAF algorithm has several versions, each requiring different computational complexity. In *Section V*, we evaluate the MB_ML using LORAF3 requiring $O(Wr_{max})$ complexity as well as LORAF1 requiring $O(Wr^2_{max})$.

B. Proposed Replica Generation for Channel Estimation

The idea of turbo channel estimation is to increase the reference signals by exploiting the LLR of the transmitted sequence fed back from the decoder. In TEQ-ACC, however, it is difficult to reproduce the soft replica for the parity (accumulated) bits which is needed in (4) and (5) from the *a posteriori* LLR λ^p_{DEC} fed back from the decoder, since it is sent only every P_a-th bits, and furthermore, the channel decoder produce the *a posteriori* LLR λ^p_{DEC} only for the doped (un-accumulated) bits. Hence, we may replace the LLR for the parity bits with zero, as

$$\lambda^a_{EST}(k) \quad = \quad \begin{cases} \lambda^p_{DEC}(k) & k \mod P_a \not\equiv 0 \\ 0 & k \mod P_a \equiv 0 \end{cases}, \qquad (10)$$

where $k = \Pi(i)$ with i being the bit index.

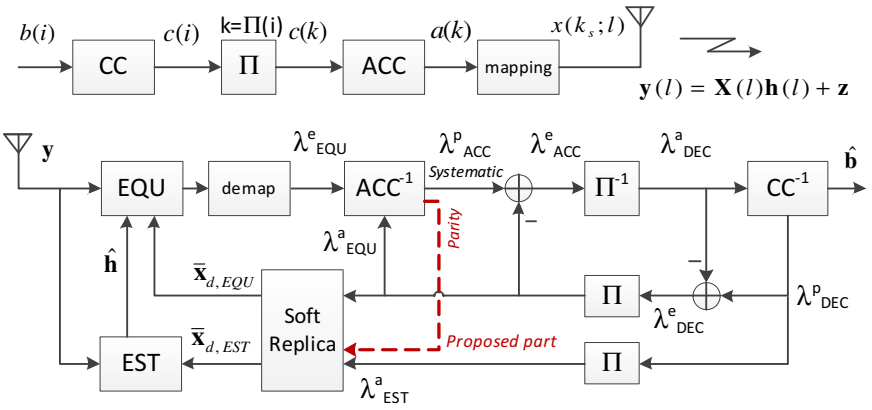

Fig. 1. System Model

We propose a new technique for recovering the LLR by using the *a posteriori* LLR of the parity bits $\lambda_{ACC}^{p,parity}$, obtained as the output of the de-accumulator, as

$$\lambda_{EST}^{a}(k) = \begin{cases} \lambda_{DEC}^{p}(k) & k \bmod P_a \not\equiv 0\,, \\ \lambda_{ACC}^{p,parity}(k) & k \bmod P_a \equiv 0\,. \end{cases} \quad (11)$$

We then generate the soft replica of transmitted symbols $\bar{x}_d(k_s)$ for SB_ML by utilizing (10) or (11). In the case of gray-mapped QPSK,

$$\bar{x}_d(k_s) = \frac{1}{\sqrt{2}}\left(\tanh\frac{\lambda_{EST}^{a}(2k)}{2} + j\tanh\frac{\lambda_{EST}^{a}(2k+1)}{2}\right) \quad (12)$$

with $j = \sqrt{-1}$, as described in [10].

IV. Exit Analysis

This section shows the effect of the doped accumulator on the extrinsic information transfer (EXIT) curve of the equalizer when the receiver actually estimates the channel in the framework of turbo equalization. For the sake of simplicity, we assume $\lambda_{EQU}^{a}(k) = \lambda_{EST}^{a}(k)$ for all k in this section.

The doped accumulator lifts up the equalizer's EXIT curve around the value range near $I_{EQU}^{a} = 1$, while it has an negative impact that it pushes down the curve around the value range near $I_{EQU}^{a} = 0$. The amount of the lift-up / push-down depends on the doping rate P_a. Hence P_a should be adjusted properly. Fig. 2 depicts the EXIT chart with the ideal channel estimation in AWGN 1-path channel at $E_b/N_0 = (2\sigma_z^2 R_c)^{-1}$ = 2 dB, to demonstrate the characteristic of the EXIT curve with the doped accumulator. Around the value range near $I_{EQU}^{a} = 0$, the equalizer's EXIT curve with $P_a = 16$ is closer to that without doped accumulator than with $P_a = 8$. However the equalizer's EXIT curve with $P_a = 16$ intersects with the decoder's EXIT curve around the value range near $I_{EQU}^{a} = 0.9$. It is expected that the trajectories of turbo equalization with the doped accumulator with $P_a = 4, 8$ reach the (1,1) mutual information (MI) point. Whereas without the doped accumulator, trajectories do not reach the (1,1) MI point since the two EXIT curves intersect in this case.

The doping rate P_a should, therefore, be adjusted so that the two curves keep reasonable gap over the entire range of

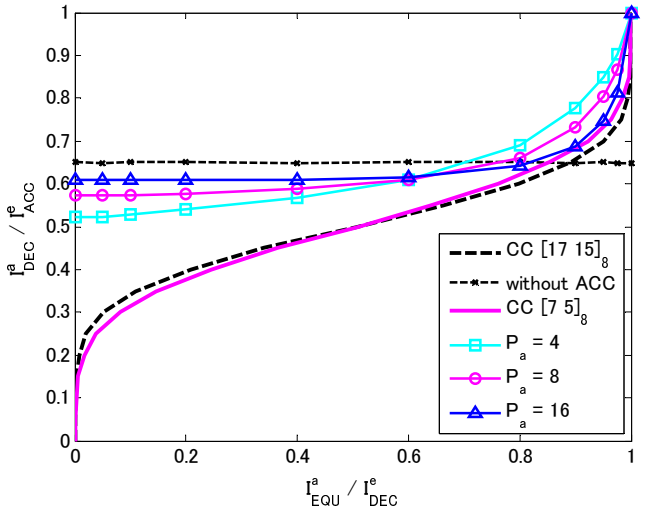

Fig. 2. EXIT Chart (Known H, 1 ANT) : AWGN 1-path, E_b/N_0 = 2 dB

I_{EQU}^{a}, where account should be taken of the impact of the channel estimation error. Fig. 3 shows the EXIT chart for turbo equalization in a fading channel realization (6-paths having equal average power) with SB_ML and MB_ML. MB_ML can lift the equalizer's EXIT curve up even though equalizer's *a priori* information is not high enough. However it should be noticed that the EXIT curves with SB_ML also needs to keep the reasonable gap since MB_ML utilizes the estimation results obtained with SB_ML as we can see in the equation (6). Fig. 3 thereby suggests that $P_a = 8$ is suitable in this fading channel rather than $P_a = 4$.

V. Simulations

This section presents computer simulation results to show the performance of TEQ-ACC when the receiver actually estimates the channel impulse response. The performance of TEQ-ACC is compared with TEQ-CVT. Both the transmission systems employ the convolutional code with coding rate $R_c = 1/2$ and the same memory length in total. TEQ-ACC employs a memory 2 convolutional coding with $(g1, g2) = (7, 5)_8$, and

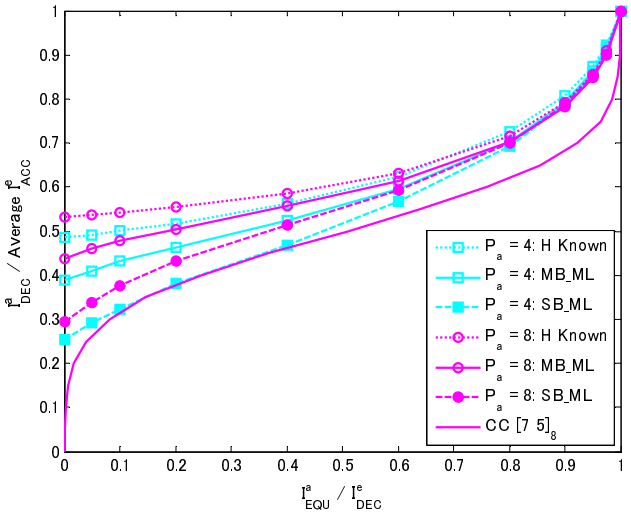

Fig. 3. EXIT Chart: 1 ANT, fading 6 paths, average E_b/N_0 = 4 dB

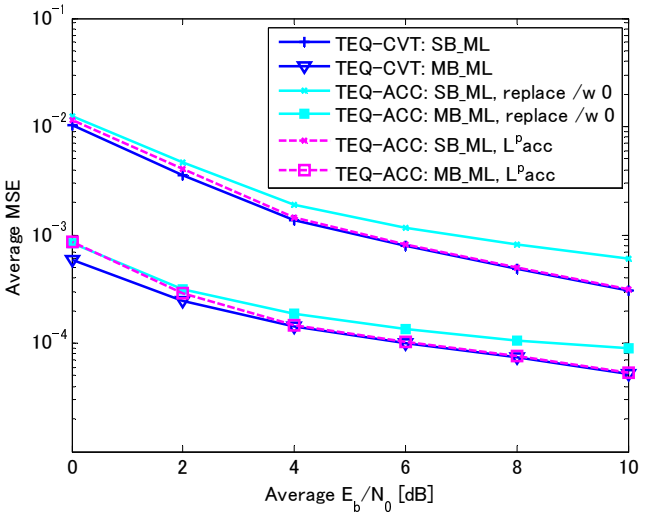

Fig. 5. MSE of channel estimate in PB3, 6 iterations, 2 ANT

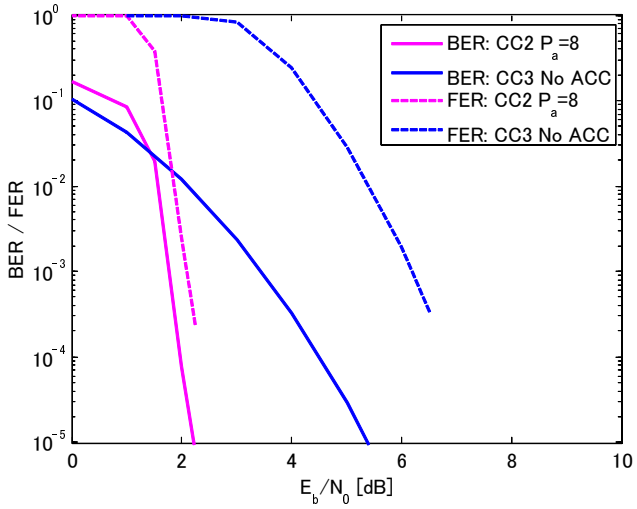

Fig. 4. BER and FER in 1-path AWGN, 36 iterations, 1 ANT

the doped accumulator with memory length = 1 and the doping rate $P_a = 8$. On the other hand, TEQ-CVT employs a memory 3 convolutional code with $(g1, g2) = (17, 15)_8$. The parameters of the frame structure are $N_d = 480$, $N_t = N_{CP} = 32$ symbols and $N_B = 5$ bursts.

Fig. 4 shows BER and FER of the receivers with TEQ-ACC and TEQ-CVT in the 1-path AWGN channel. Since the purpose of Fig. 4 is to compare the basic performances of turbo equalization with and without the doped accumulator, the ideal channel estimation is assumed. Each receiver has a single antenna and performs 36 iterations. We observe TEQ-ACC achieves more than 3 dB gain at BER = 10^{-5} and 4 dB gain at FER = 10^{-3} over TEQ-CVT.

A. Comparison in a model based fading channel

Fig. 5 shows the average mean square error (MSE) of channel estimation in 6 paths fading channels of which realizations follow the Pedestrian-B model with 3 km/h (PB3) mobility assumptions [11]. The carrier frequency $f_c = 2$ GHz and the sampling interval $T_s = 0.2$ μsec. The receivers have two antennas and perform 6 iterations. In this case, the MSE of channel estimation with TEQ-ACC using the replica generation by (10) is inferior to that with TEQ-CVT, even though using the multi burst channel estimation technique with the window length $L = 300$. However, the MSE of channel estimation with TEQ-ACC using the replica generation defined by (11) converges into the MSE of TEQ-CVT as E_b/N_0 increases. Therefore it can be concluded that the proposed replica generation method (11) can reduce the negative impact of the losing soft information due to doping. We henceforth evaluate TEQ-ACC with the proposed method (11) alone in the following sections. Fig. 6 shows BER and FER with TEQ-ACC and TEQ-CVT, respectively, in the PB3 channel. The gain with TEQ-ACC over TEQ-CVT is very minor at BER = 10^{-5}. However FER with TEQ-ACC using MB_ML is roughly 1 dB better than that of TEQ-CVT at FER = 10^{-3}, including the impact of channel estimation error.

B. Verification in a realistic propagation scenario

We then verify the TEQ-ACC when it is combined with the channel estimation utilizing practical subspace tracking techniques in a realistic channel scenario based on measurement data. The measurement campaign took place at the court yard of Technical University of Ilmenau in Germany. Fig. 7(a) shows the variation of path power, and (b) shows the position index where the peak of the impluse response exists. The channel impulse response data gathered by the RUSK channel sounder [12] shows that the peak position changes quite frequently, which does not happen with the model-based simulations such as PB3 channel. The channel obtained in the field measurement has up to 30 symbols of ISI. Average power control was assumed. The sounder's transmitter moved at a pedestrian speed.

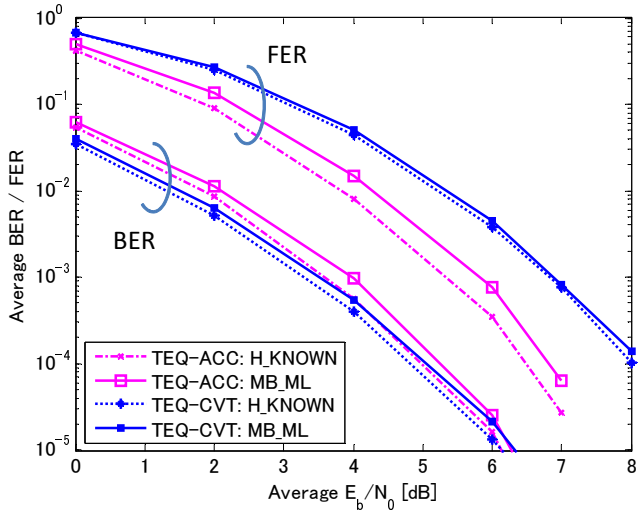

Fig. 6. BER and FER in PB3, 6 iterations, 2 ANT

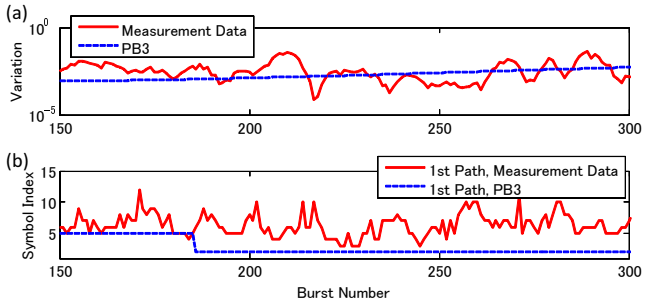

Fig. 7. An example of analysis of the channel impulse response: (a) Variation of Path Power $\mathrm{var}\{\mathtt{diag}(\mathbf{h}(l)\mathbf{h}^H(l))\}$, (b) Peak Path Position

Figs. 8(a) and (b) show the means square error (MSE) of channel estimation and the results of the rank estimation corresponding to the dominant subspace, respectively, obtained by using the realistic channel impulse response. The channel estimation techniques ML_MB with SVD and with LORAF1 reduce MSE effectively than ML_SB. ML_MB with LORAF3 fails improving MSE during the first several hundred of bursts. However it should be noticed that LORAF3 also improves MSE after the initial duration which is equivalent to the multi burst window length $L = 300$. During this duration, LORAF3 mainly works for initializing the internal memory, in exchange for reducing the computational complexity from $O(Wr_{max}^2)$ needed with LORAF1 to $O(Wr_{max})$. We thereby start using the projection matrix $\hat{\mathbf{P}}$ computed by LORAF3 after the initialization, and until then we set $\hat{\mathbf{P}}$ as an identity matrix in the equation (6). Fig. 9 shows FER performance with TEQ-ACC and TEQ-CVT, in the realistic propagation scenario using the measurement data. Similarly to the results in the PB3, the FER gain with TEQ-ACC over TEQ-CVT, both using MB_ML, is 1 dB at FER = 10^{-3}. It should be emphasized that TEQ-ACC combined with MB_ML channel estimation using LORAF3 subspace tracking technique achieved exactly the same FER performance as the one using the sliding window SVD-based technique.

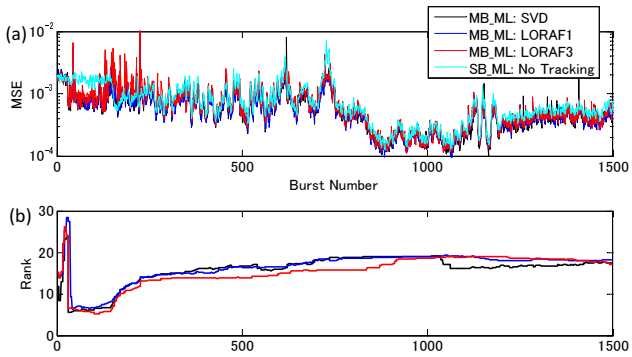

Fig. 8. (a) MSE of channel estimate, (b) Rank Estimation: TEQ-ACC, 6 iterations, Average E_b/N_0 = 7 dB, Measurement data

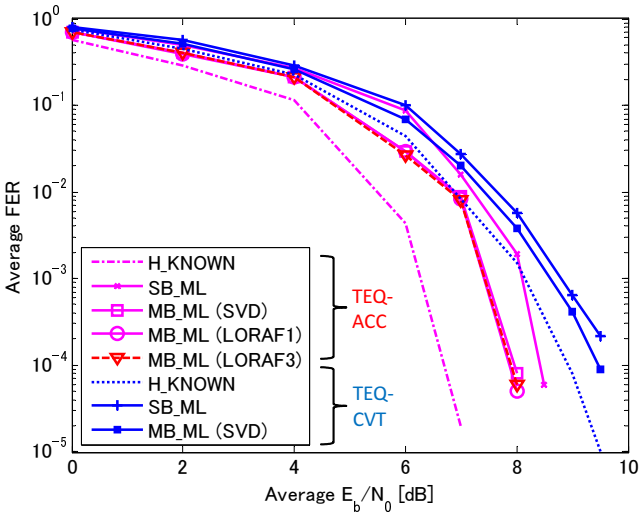

Fig. 9. FER in the propagation scenario based on the measurement data

VI. Conclusion

This paper has revealed the performance of the turbo equalization using doped accumulator (TEQ-ACC) when it is combined with channel estimation in the realistic propagation scenario using the measurement data as well as in model-based frequency selective fading channels. It has been shown that the MSE of channel estimation in TEQ-ACC is inferior to that with the conventional turbo equalization without doped accumulator (TEQ-CVT), if TEQ-ACC generates the soft replica for the channel estimation only from the *a posteriori* LLR fed back from the decoder.

This paper proposed a new replica generation method, effective with the combined use of the doped accumulator, which utilizes the *a posteriori* LLR produced by the de-accumulator as well as that fed back from the decoder. It has been shown that the proposed technique can reduce the impact of the channel estimation error in TEQ-ACC. It

was then demonstrated that the channel estimation using the proposed replica generation method in TEQ-ACC achieves asymptotically the equivalent channel estimation accuracy in terms of MSE to that with TEQ-CVT as E_b/N_0 increases. Simulation results showed that TEQ-ACC with the proposed soft replica generation method for channel estimation achieves roughly 1 dB gain at FER = 10^{-3} over TEQ-CVT in channel scenarios with pedestrian mobility assumptions.

Furthermore, through computer simulations, this paper has verified the effectiveness of TEQ-ACC with the adaptive channel estimation using the subspace tracking techniques LORAF1 and LORAF3 in the realistic propagation scenario based on the measurement data. TEQ-ACC with channel estimation using LORAF3 achieves exactly the same FER performance with one using the sliding window SVD-based technique, while reducing the computational complexity from $O(W^3)$ to $O(Wr_{max})$ where W is ISI length with $r_{max} \leq W$ being a pre-defined constant.

REFERENCES

[1] K. Anwar and T. Matsumoto, "Very Simple BICM-ID Using Repetition Code and Extended Mapping with Doped Accumulator," *Wireless Personal Comm., Springer, DOI 10.1007/s11277-011-0397-1, published online on 13 Sep. 2011*.

[2] ——, "Low Complexity Time-Concatenated Turbo Equalization for Block Transmission without Guard Interval: Part 1 - The Concept," *Submitted to Wireless Personal Comm., Springer*.

[3] P. Strobach, "Low-rank adaptive filters," *Signal Processing, IEEE Trans. on*, vol. 44, no. 12, pp. 2932–2947, Dec. 1996.

[4] K. Kansanen, "Wireless broadband single-carrier systems with MMSE turbo equalization receivers," *University of Oulu, Oulu Finland*, 2005.

[5] L. Bahl, J. Cocke, F. Jelinek, and J. Raviv, "Optimal decoding of linear codes for minimizing symbol error rate (Corresp.)," *Information Theory, IEEE Trans. on*, vol. 20, no. 2, pp. 284 – 287, Mar. 1974.

[6] M. Nicoli, S. Ferrara, and U. Spagnolini, "Soft-Iterative Channel Estimation: Methods and Performance Analysis," *Signal Processing, IEEE Trans. on*, vol. 55, no. 6, pp. 2993 –3006, 2007.

[7] M. Wax and T. Kailath, "Detection of signals by information theoretic criteria," *Acoustics, Speech and Signal Processing, IEEE Trans. on*, vol. 33, no. 2, pp. 387 – 392, Apr. 1985.

[8] L. N. Trefethen and I. David Bau, "Numerical Linear Algebra," *SIAM*, 1997.

[9] S. Ferrara, T. Matsumoto, M. Nicoli, and U. Spagnolini, "Soft Iterative Channel Estimation With Subspace and Rank Tracking," *Signal Processing Letters, IEEE*, vol. 14, no. 1, pp. 5–8, 2007.

[10] M. Tuchler, R. Koetter, and A. Singer, "Turbo equalization: principles and new results," *Comm., IEEE Trans. on*, vol. 50, no. 5, pp. 754 –767, may 2002.

[11] 3rd Generation Partnership Project, "3GPP TR25.996, Spatial Channel Model for MIMO Simulations (Release 6)."

[12] http://www.channelsounder.de/.